Acta Crystallographica Section D
Biological Crystallography
ISSN 0907-4449

Crystallographic studies of the interaction between the ferredoxin-NADP$^+$ reductase and ferredoxin from the cyanobacterium *Anabaena*: looking for the elusive ferredoxin molecule

Renaud Morales, Galina Kachalova,† Frédéric Vellieux, Marie-Hélène Charon and Michel Frey*

LCCP, Institut de Biologie Structurale J. P. Ebel, CEA–CNRS, 41 Rue Jules Horowitz, F38027 Grenoble, France

† Present address: Max-Planck-Institut, Notkestrasse 85, 22603 Hamburg, Germany.

Correspondence e-mail: frey@lccp.ibs.fr

Received 5 June 2000
Accepted 19 July 2000

PDB Reference: Anabaena PCC7119 ferredoxin–ferredoxin-NADP$^+$ reductase complex, 1ewy.

Ferredoxin-NADP$^+$ reductase (FNR) and its physiological electron donor ferredoxin (Fd) from the cyanobacterium *Anabaena* PCC7119 have been co-crystallized. The unit-cell parameters are $a = b = 63.72$, $c = 158.02$ Å and the space group is $P2_12_12_1$. The crystal structure has been solved with 2.4 Å resolution synchrotron data by molecular replacement, anomalous dispersion and $R_{\rm min}$ search methods. For the computations, the crystal was treated as a merohedral twin. The asymmetric unit contains two FNR molecules and one ferredoxin molecule. The packing of the FNR molecules displays a nearly tetragonal symmetry (space group $P4_32_12$), whereas the ferredoxin arrangement is orthorhombic. This study provides the first crystallographic model of a dissociable complex between FNR and Fd.

1. Introduction

Ferredoxin-NADP$^+$ reductases are FAD flavoproteins that catalyze the reduction of nicotinamide-adenine dinucleotide phosphate (NADP$^+$) to NADPH during photosynthesis in higher plants, algae and cyanobacteria. They accomplish this process by mediating the transfer of two electrons from photosystem I to NADP$^+$ *via* a [2Fe–2S] ferredoxin in two successive one-electron steps (reviewed by Arakaki *et al.*, 1997). Electron transfer between ferredoxin and FNR requires the formation of a ternary NADP$^+$–FNR–Fd complex (Batie & Kamin, 1984; Sancho & Gómez-Moreno, 1991). The crystal structures of the individual FNR [in its oxidized state (Serre *et al.*, 1996) and reduced state (unpublished data)] and Fd (also in both redox states; Morales *et al.*, 1999) from the cyanobacterium *Anabaena* PCC7119 have been determined. Here, we report the co-crystallization of the two physiological protein partners FNR and ferredoxin from the same organism. The aim of this study was to provide a structural basis for further understanding of the catalytic mechanism of NADP$^+$ reduction during photosynthesis and, more generally, of protein–protein interactions and intermolecular electron-transfer processes.

2. Materials and methods

2.1. Crystallization and characterization

Ferredoxin and FNR from the cyanobacterium *Anabaena* PCC7119 were purified separately as described previously (Pueyo & Gómez-Moreno, 1991). Crystals containing Fd and FNR were obtained by vapour-diffusion techniques at 293 K in hanging drops, under conditions similar to those used to grow the original FNR crystals in solutions devoid of salt (Serre *et al.*, 1996), with an excess of FNR over Fd. The protein

solution contained 0.7 m*M* oxidized FNR, 0.5 m*M* oxidized Fd buffered with 0.1 *M* Tris–HCl pH 8.0; the reservoir solution contained 0.1 *M* MES pH 5.5, 18–21%(*w*/*v*) PEG 6000 and 0.1%(*w*/*v*) sodium azide. The droplet was initially formed by mixing 2 µl of the reservoir solution, 1 µl of a 5% β-octyl glucoside solution and 2 µl of the protein solution. The crystals grow as red–orange tetragonal bipyramids (0.1 × 0.1 × 0.3 mm), sometimes together with yellow hexagonal bipyramid crystals typical of native FNR crystals (Fig. 1). This red–orange colour of the crystals gave the first indication that they contained ferredoxin. In any case, the crystals were difficult to obtain reproducibly.

2.2. Crystallographic characterization and localization of the FNR and Fd molecules

Prior to X-ray data collection, a crystal was soaked in the reservoir solution with 20% glycerol added. The diffraction intensities were collected at 100 K on a MAR Research image-plate detector to 2.38 Å resolution with λ = 0.98 Å at the European Synchrotron Radiation Facility (ESRF beamline ID2) in Grenoble. The crystal appeared to belong to the tetragonal space group $P4_22_12$, with unit-cell parameters $a = b = 63.7$, $c = 158.0$ Å and the general reflection conditions $h00$, $h = 2n$; $0k0$, $k = 2n$; $00l$, $l = 2n$. The data were processed in the point group 4/*mmm* with the *MOSFLM* (Leslie, 1991), *SCALA* and *TRUNCATE* programs (Collaborative Computational Project, Number 4, 1994; Table 1). Attempts to position the FNR and Fd molecules with 10–3.5 Å resolution data by molecular replacement with *AMoRe* (Navaza, 1994) and the *Anabaena* PCC7119 oxidized FNR and Fd X-ray models (Serre *et al.*, 1996; Morales *et al.*, 1999) were unsuccessful. However, the $00l$, $l = 4n$ reflections were far stronger ($|F| = 60\sigma$) and $00l$, $l = 4n + 2$ reflections weaker ($|F| = 5\sigma$) than the average reflection ($|F| = 8\sigma$). Therefore, we attempted to position the FNR and Fd molecules with *AMoRe* (Navaza, 1994) for the two enantiomorphic space groups $P4_12_12$ or $P4_32_12$, for which the $00l$ reflection condition is $l = 4n$. This time, we easily positioned one FNR molecule in the asymmetric unit for the space group $P4_32_12$ (with data in the resolution range 10–3.5 Å; $R = 0.39$, CC = 0.55). The resulting electron-density map of FNR was clearly interpretable, except for some stretches corresponding to the putative ferredoxin-binding zone. By contrast, we could not locate any ferredoxin molecule, either by $\sigma_A\, 2\rho_o - \rho_c$ or $\rho_o - \rho_c$ maps using phases calculated from the refined position of the FNR ('FNR phases') or by molecular replacement.

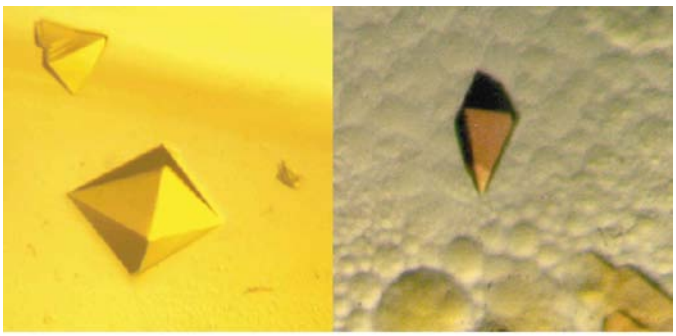

(*a*) (*b*)

Figure 1
Crystals of (*a*) FNR (0.5 × 0.5 × 0.5 mm) and (*b*) Fd–FNR (0.1 × 0.1 × 0.3 mm).

Table 1
X-ray data collection and processing statistics.

Numbers in parentheses represent the value for the highest resolution shell (2.38–2.5 Å).

Radiation source	ESRF (ID2)†	
Wavelength (Å)	0.98	
Resolution range (Å)	40.0–2.38	
Point group	4/*mmm*	*mmm*
Unit-cell dimensions (Å)	63.72, 63.72, 158.02	63.72, 63.73, 158.02
Unique reflections	13278	25838
Completeness (%)	98.2 (93.6)	97.2 (87.7)
Multiplicity	8.2 (6.7)	4.3 (3.7)
$I/\sigma(I)$	7.2 (6.7)	7.9 (7.3)
R_{sym}‡ (%)	5.4 (8.8)	4.6 (7.7)

† European Synchrotron Radiation Facility, Grenoble, France. ‡ $R_{sym} = \sum|I_h - \langle I_h\rangle|/\sum I_h$, where $\langle I_h\rangle$ is the average of equivalent reflections.

2.3. Localization of the ferredoxin molecule

A Fourier map was then calculated using the anomalous amplitudes and 'FNR phases'. In this map, two well resolved peaks (above 4σ) were observed in the asymmetric unit (Fig. 2*a*), which were assigned to the two Fe atoms (named Fe1 and Fe2) of a ferredoxin [2Fe–2S] cluster since (i) their separation (2.75 Å) was comparable to that observed in the [2Fe–2S] cluster of the PCC7119 Fd (Morales *et al.*, 1999) and (ii) they were close to the FAD C8M of the FNR (7.4 Å) as predicted by biochemical and biophysical experiments (Walker *et al.*, 1991).

To position the Fd molecule, the Fd model was manually rotated on a graphic display using *O* (Jones *et al.*, 1991) around the Fe1–Fe2 axis, keeping the two Fe atoms of the [2Fe–2S] cluster superimposed on the two anomalous peaks. One of the two possible assignations (*i.e.* Fe1 Fe2 or Fe2 Fe1) of the Fe atoms to these anomalous peaks was quickly discarded because it led to extensive overlaps between Fd and FNR. For the second assignation, the Fd was rotated in steps of 5° and in each step the complex between the FNR and the rotated Fd was refined by rigid-body minimization with *X-PLOR* (Brünger, 1992*a*). The corresponding R and R_{free} factors (Brünger, 1992*b*) fell sharply and significantly within a narrow range of the Fd rotation angle (30°; Fig. 2*b*). All the Fd positions obtained within this angular range were identical. However, this optimal (R_{min}) position (coloured red in Fig. 2*c*) intersected with the crystallographic dyad axis [110] so that it extensively overlapped with a symmetry-related Fd (coloured blue). At this stage, crystal packing analysis showed that the crystal contained twice as many FNR as Fd molecules, with a V_M of 1.96 Å^3 Da^{-1} (Matthews, 1968). Therefore, the symmetry of the Fd packing within the crystal could not be tetragonal.

When the weak reflections $l = 4n + 2$ are taken into account, the general reflection conditions ($h00$, $h = 2n$; $0k0$, $k = 2n$; $00l$,

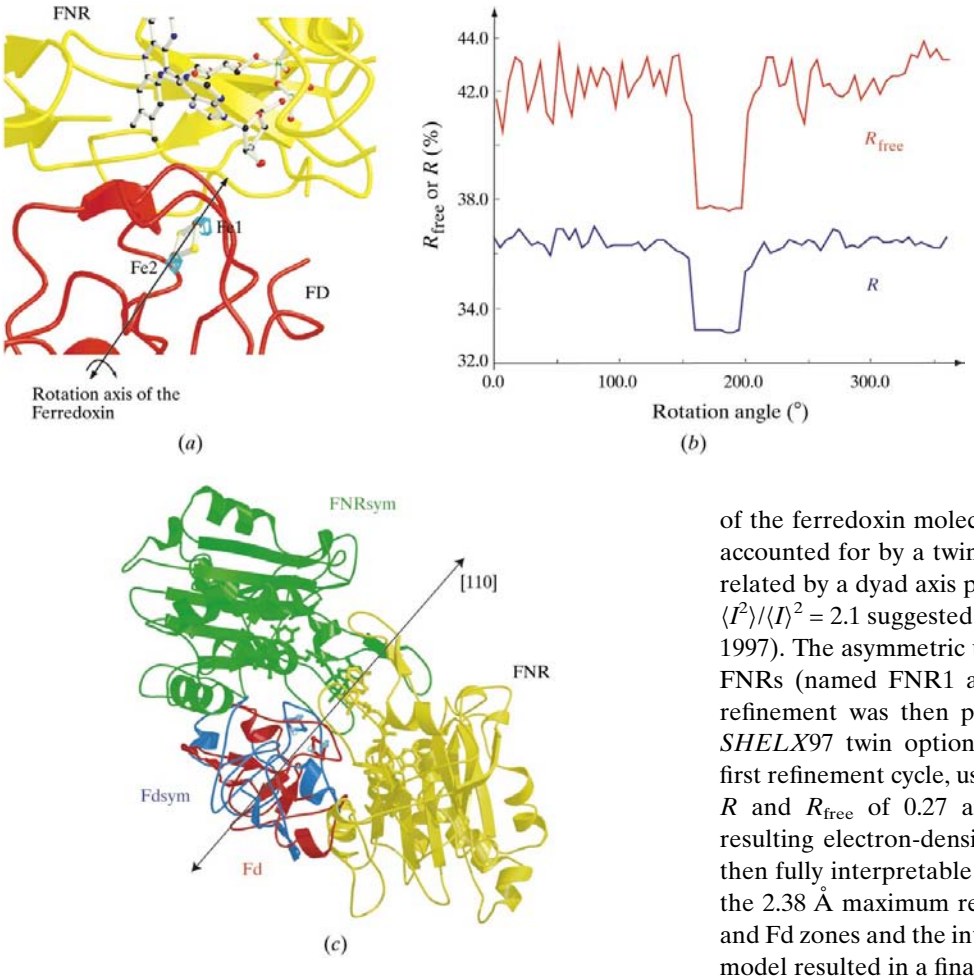

Figure 2
(*a*) Localization of the ferredoxin; the [2Fe–2S] cluster Fe atoms are superimposed with the anomalous peaks (in blue). (*b*) R (blue) and R_{free} (red) factors values as a function of the rotation angle (the origin is arbitrary) of the ferredoxin around the Fe1–Fe2 axis. (*c*) Ribbon diagram of the two FNR (green–yellow) and Fd (blue and red) molecules related by the dyad axis [110] in the tetragonal space group.

$l = 2n$) could also correspond to the orthorhombic space group $P2_12_12_1$. Accordingly, our X-ray data set were re-indexed for an *mmm* point group. Using these reindexed data, two FNR molecules were easily positioned within the $P2_12_12_1$ asymmetric unit by molecular replacement with *AMoRe* (Navaza, 1994) (for 10–3.5 Å resolution data, R = 0.39, CC = 0.54). These two FNR positions are related to their corresponding positions in the tetragonal cell by a ($-\frac{1}{4}$, 0, $-\frac{1}{8}$) translation vector.

However, no position for any Fd molecule could be found within the $P2_12_12_1$ asymmetric unit either by molecular replacement or by Fourier calculations using the 'FNR phases'. Therefore, the ferredoxin molecule was positioned in the orthorhombic asymmetric unit by translating one of the two ferredoxins, symmetry-related by the [110] crystallographic axis in the tetragonal cell, by a vector ($\frac{1}{4}$, 0, $\frac{1}{8}$). Following a new round of refinement cycles of a model including the two FNRs and this Fd (using data in the resolution range 10–3 Å; R = 0.36 and R_{free} = 0.36), an electron-density map was obtained in which the density of the ferredoxin was visible. However, the map was not interpretable owing to the presence of an overlapping density related by a pseudo-dyad axis parallel to [110]. Not surprisingly, the same results were obtained for the other possible position of the ferredoxin.

2.4. Twin refinement

This prompted us to consider that the two possible orientations of the ferredoxin molecule in the orthorhombic cell might be accounted for by a twinned crystal with the twin components related by a dyad axis parallel to [110], even though the ratio $\langle I^2\rangle/\langle I\rangle^2 = 2.1$ suggested that the data were untwinned (Yeates, 1997). The asymmetric unit of each component contained two FNRs (named FNR1 and FNR2) and one Fd (Fig. 3). The refinement was then performed against intensities with the *SHELX*97 twin option (Sheldrick & Schneider, 1997). The first refinement cycle, using 15–2.5 Å resolution data, led to an R and R_{free} of 0.27 and 0.33, respectively (Table 2). The resulting electron-density map of the two FNRs and Fd was then fully interpretable (Fig. 4). Stepwise extension of data to the 2.38 Å maximum resolution, remodelling of several FNR and Fd zones and the introduction of 91 water molecules in the model resulted in a final R = 0.22 and R_{free} = 0.29. The refined fractional contribution of each twin component was 0.5. Refinement statistics are given in Table 2.

2.5. Quality and analysis of the model

The final electron-density map accounts for the FNR and Fd chemical sequences except for residues 1–10 of both FNR1 and FNR2 and residue 68 and the side chain of Asp62 of Fd, the electron densities of which are not visible. This lack of density probably reflects the known flexibility of the FNR N-terminal region (*e.g.* Serre *et al.*, 1996), which points to the solvent channels, and the disorder of some ferredoxin residues in direct contact with FNR1. It is of interest to note that in contrast to the X-ray studies of the individual FNR or of its complex with $NADP^+$ (Serre *et al.*, 1996), the electron density of the loop 106–112 is well defined. It should also be pointed out that the ferredoxin electron density is well defined, although its average B factor is very high (65 $Å^2$; Fig. 4; Table 2). In comparison with the uncomplexed structures (Serre *et al.*, 1996; Morales *et al.*, 1999), the FNR conformational changes are a consequence of the FNR packing in the asymmetric unit and do not involve any residue interacting with Fd, whereas the Fd changes only result from a strong interaction with FNR1, particularly through Ser64 and Phe65. The ferredoxin is not involved in crystal packing interactions. Futhermore, the interactions between Fd and FNR1 are more

Table 2
Refinement statistics.

Resolution range (Å)	15.0–2.38
R (%)/No. reflections	21.9/23138
R_{free}† (%)/No. reflections	29.2/2563
Number of atoms	5633
Number of water molecules	91
Average B value (Å^2)	50
Average B value for FNR1 (Å^2)	46
Average B value for FNR2 (Å^2)	47
Average B value for Fd (Å^2)	65
R.m.s.d.‡ from ideality	
Bond length (Å)	0.022
Bond angle (Å)	0.022
Ramachandran plot	
Favoured (%)	81.5
Allowed (%)	17.5
Generous (%)	0.9
Disallowed (%)	0.2

† Based on 10% of the data randomly selected. ‡ Root-mean-square deviation.

specific than those between Fd and FNR2 or those between FNR1 and FNR2 in terms of possible hydrogen bonds (Table 3).

2.6. *A posteriori* molecular-replacement calculations

As two FNR molecules (molecular weight 2 × 35 kDa) and one Fd molecule (MW = 11 kDa) are present in the asymmetric unit, the contribution of Fd to the diffraction pattern is rather weak (about one-sixth of the scattering matter). This probably explains the failure of the *ab initio* molecular-replacement calculations. To check this hypothesis, rotation-function calculations were resumed, this time using the difference amplitude values $|\Delta|$ corresponding to the scattering of the Fd component alone. The set of these $|\Delta|$ values (1274 data in the resolution range 10.0–6.0 Å) was obtained by subtracting the calculated FNR structure factors $|F_{calc}|$, properly scaled to take into account their contribution to the diffraction pattern (*i.e.* about 5/6), from the observed amplitudes $|F_{obs}|$. The resulting $|\Delta| = |F_{obs}| - 0.85|F_{calc}|$ were then truncated by eliminating all difference amplitudes larger than a cutoff value of 300.0 to provide the data set used for rotation-function calculations (891 $|\Delta|$ values). The rotation-function calculations were carried out using Crowther's fast rotation function (Crowther, 1972). The Fd search model was placed at the origin of an orthorhombic $P1$ cell of dimensions 70 × 70 × 70 Å. The limiting radii used during the computations were 6.0 and 35.0 Å. The calculations showed a solution in section $\beta = 15^\circ$ as the third peak of the rotation function and the top peak in this section (Rf value = 108, maximum = 129, mean Rf value = 3) which only differed from the previous solution by 5° along both β and γ.

The rotated search model was then used for translation-function calculations with the program *BRUTE* (Fujinaga & Read, 1987), keeping the two FNR molecules fixed. This allowed the translation search to be undertaken using the measured set of $|F_{obs}|$ (in the resolution range 10.0–4.0 Å) instead of the $|\Delta|$ values used in the previous step. The

Table 3
Fd–FNR1, Fd–FNR2 and FNR1–FNR2 interactions in the asymmetric unit.

	Fd–FNR1	Fd–FNR2	FNR1–FNR2
No. hydrogen bonds†	12	3	3
No. van der Waals contacts (<4.1 Å)	54	21	45
Buried surface (Å^2)	1600	1100	1600

† $D\cdots A$ distance < 3.4 Å; D—H$\cdots A$ > 90°.

Figure 3
Content of the asymmetric unit of each twin component. The ferredoxin (Fd) is coloured red and the FNR molecules (FNR1 and FNR2) yellow and green. The corresponding redox centres, FAD isoalloxazines and the [2Fe–2S] cluster lozenge are represented in the same colours. FNR1 and FNR2 are symmetry-related by a dyad axis except for the zones of their surface in contact with the ferredoxin (not shown in detail). The Fd–FNR1 association mimics a biologically relevant Fd–FNR electron-transfer complex.

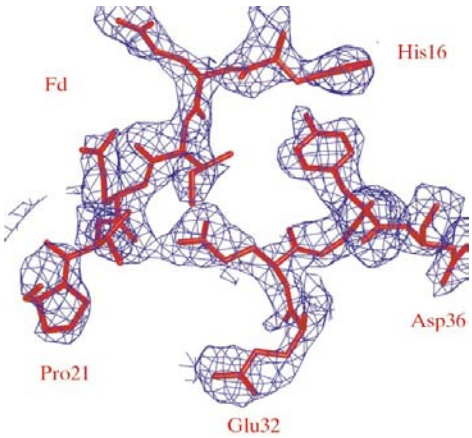

Figure 4
A typical view of the electron density of the Fd molecule after 'twin' refinement.

translation-function calculations were carried out in a series of three searches over intersecting planes, each search using only the symmetry operations corresponding to one of the 2_1 screw axes in space group $P2_12_12_1$. However, the three translation sections showed many resolved peaks. Therefore, to rapidly select the translation vector we used the positions of the [2Fe–2S] cluster Fe atoms that had previously been obtained from anomalous dispersion maps.

3. Discussion

Crystals containing FNR and Fd could only been obtained with an excess of FNR over Fd in the crystallization solutions (FNR:Fd molar ratio of 1.4 or 2). This is reminiscent of the co-crystallization of yeast cytochrome *c* peroxidase (CCP) complexed with horse heart cytochrome *c* [cc(H)] [CCP/cc(H) ratio = 2.0; Pelletier & Kraut, 1992] and more recently of a complex between one domain of the *Staphyloccoccus aureus* protein A and a human antibody Fab fragment (Graille *et al.*, 2000). Under these conditions, the presence of a moiety containing two FNR molecules per ferredoxin in the asymmetric unit is not surprising. It follows that the ferredoxin (Fd) makes little contribution to the overall X-ray scattering. This explains the difficulties experienced in locating Fd within the crystal, which is further complicated by the packing of the FNR molecules showing a nearly tetragonal symmetry, whereas the Fd molecule packing is orthorhombic.

The modelling of the crystal as a twin, at odds with the statistical analysis, proved to be a very powerful tool in obtaining fully interpretable electron-density maps of the ferredoxin. It is of interest to note that a similar strategy has been recently used to refine a RNA heptamer double helices (Mueller *et al.*, 1999). However, the possibility that the asymmetric unit actually contains two FNR1–FNR2–Fd moieties with two possible orientations around [110] cannot be excluded. This would imply that the *c* parameter is doubled (*i.e.* 316 Å).

Within the asymmetric unit, the interactions between Fd and FNR1 (Fd/FNR1; Table 3) are quite comparable to those observed in other biologically relevant crystallographic complexes (Pelletier & Kraut, 1992; Lo Conte *et al.*, 1999). Moreover, a body of biological and biophysical studies in solution (*e.g.*Walker *et al.*, 1991; Hurley *et al.*, 1997; Martínez-Júlvez *et al.*, 1998 and citations therein) strongly suggests that this Fd–FNR1 association could mimic a catalytically competent electron-transfer complex between Fd and FNR. Although the association of Fd and FNR2 or the crystallographic moiety Fd–FNR1–FNR2 are more extended than for usual crystal packing interactions (Janin, 1997), they cannot be considered to be functionally relevant (Table 3). Fd–FNR2 cannot represent an efficient electron-transfer complex because the two redox centres are too far away from each other (14.5 Å). Moreover, the FNR1–Fd–FNR2 moiety has to be considered merely as a crystallization artefact as the FNR1 and FNR2 $NADP^+$ binding sites are buried.

The figures were produced with *MOLSCRIPT* (Kraulis, 1991), *BOBSCRIPT* (Esnouf, 1997) and *Raster3D* (Merritt & Bacon, 1997).

We thank Drs Bjarne Rasmussen, Julien Lescar and Xavier Vernède for their help in collecting synchrotron data at ESRF. This work was supported by the CEA, the CNRS and a grant (RM) from the Ministère de l'Education Nationale, de la Recherche et de la Technologie.

References

Arakaki, A. K., Ceccarelli, E. A. & Carrillo, N. (1997). *FASEB J.* **11**, 133–140.
Batie, C. J. & Kamin, H. (1984). *J. Biol. Chem.* **259**, 8832–8839.
Brünger, A. T. (1992*a*). *X-PLOR Version* 3.1. *A System for X-ray Crystallography and NMR.* New Haven, CT: Yale University Press.
Brünger, A. T. (1992*b*). *Nature (London)*, **355**, 472–475.
Collaborative Computational Project, Number 4 (1994). *Acta Cryst.* D**50**, 760–763.
Crowther, R. A. (1972). *The Molecular Replacement Method*, edited by M. G. Rossmann, pp. 173–178. New York: Gordon & Breach.
Esnouf, R. M. (1997). *J. Mol. Graph.* **15**, 133–138.
Fujinaga, M. & Read, R. J. (1987). *J. Appl. Cryst.* **20**, 517–521.
Graille, M., Stura, E. A., Corper, A. L., Sutton, B. J., Tausig, M. J. & Charbonnier, J.-B. (2000). *Proc. Natl Acad. Sci. USA*, **97**, 5399–5404.
Hurley, J. K., Weber-Main, A. M., Stankovich, M. T., Benning, M. M., Thoden, J. B., Vanhooke, J. L., Holden, H. M., Chae, Y. K., Xia, B., Cheng, H., Markley, J. L., Martinez-Julvez, M., Gomez-Moreno, C., Schmeits, J. L. & Tollin, G. (1997). *Biochemistry*, **36**, 11100–11117.
Janin, J. (1997). *Nature Struct. Biol.* **4**, 973–974.
Jones, T. A., Zou, J. Y., Cowan, S. W. & Kjeldgaard, M. (1991). *Acta Cryst.* A**47**, 110–119.
Kraulis, P. J. (1991). *J. Appl. Cryst.* **24**, 946–950.
Leslie, A. G. W. (1991). *Molecular Data Processing in Crystallographic Computing*, edited by D. Moras, A. D. Podjarny & J. C. Thierry, pp. 50–61. Oxford University Press.
Lo Conte, L., Chothia, C. & Janin, J. (1999). *J. Mol. Biol.* **285**, 2177–2198.
Martínez-Júlvez, M., Medina, M., Hurley, J. K., Hafezi, R., Brodie, T. B., Tollin, G. & Gómez-Moreno, C. (1998). *Biochemistry*, **37**, 13604–13613.
Matthews, B. W. (1968). *J. Mol. Biol.* **33**, 491–497.
Merritt, E. A. & Bacon, D. J. (1997). *Methods Enzymol.* **277**, 505–524.
Morales, R., Charon, M.-H., Hudry-Clergeon, G., Pétillot, Y., Norager, S., Medina, M. & Frey, M. (1999). *Biochemistry*, **38,** 15764–15773.
Mueller, U., Muller, Y. A., Herbst-Irmer, R., Sprinzl, M. & Heinemann, U. (1999). *Acta Cryst.* D**55**, 1405–1413.
Navaza, J. (1994). *Acta Cryst.* A**50**, 157–163.
Pelletier, H. & Kraut, J. (1992). *Science*, **258**, 1748–1755.
Pueyo, J. J. & Gómez-Moreno, C. (1991). *Prep. Biochem.* **21**, 191–204.
Sancho, J. & Gómez-Moreno, C. (1991). *Arch. Biochem. Biophys.* **288**, 231–238.
Serre, L., Vellieux, F. M., Medina, M., Gomez-Moreno, C., Fontecilla-Camps, J. C. & Frey, M. (1996). *J. Mol. Biol.* **263**, 20–39.
Sheldrick, G. M. & Schneider, T. R. (1997). *Methods Enzymol.* **277**, 319–343.
Walker, M. C., Pueyo, J. J., Navarro, J. A., Gómez-Moreno, C. & Tollin, G. (1991). *Arch. Biochem. Biophys.* **287**, 351–358.
Yeates, T. O. (1997). *Methods Enzymol.* **276**, 344–358.